Separation Science and Technology
Publication details, including instructions for authors and subscription information:
http://www.informaworld.com/smpp/title~content=t713708471

Single-Equilibrium-Stage Foam Fractionation of the Divalent Oxyanions $HAsO^{2-}_3$, HPO^{2-}_4, SO^{2-}_4, and SeO^{2-}_3: Determination and Utilization of Selectivity Coefficients

Robert B. Grieves[a]; Wing-Cheung Joseph Chan[a]; Richard N. Kyle[a]
[a] COLLEGE OF ENGINEERING UNIVERSITY OF KENTUCKY LEXINGTON, KENTUCKY

To cite this Article Grieves, Robert B. , Chan, Wing-Cheung Joseph and Kyle, Richard N.(1982) 'Single-Equilibrium-Stage Foam Fractionation of the Divalent Oxyanions $HAsO^{2-}_3$, HPO^{2-}_4, SO^{2-}_4, and SeO^{2-}_3: Determination and Utilization of Selectivity Coefficients', Separation Science and Technology, 17: 5, 655 — 671
To link to this Article: DOI: 10.1080/01496398208068558
URL: http://dx.doi.org/10.1080/01496398208068558

SEPARATION SCIENCE AND TECHNOLOGY, 17(5), pp. 655–671, 1982

Single-Equilibrium-Stage Foam Fractionation of the Divalent Oxyanions $HAsO_4^{2-}$, HPO_4^{2-}, SO_4^{2-}, and SeO_3^{2-}: Determination and Utilization of Selectivity Coefficients

ROBERT B. GRIEVES, WING-CHEUNG JOSEPH CHAN, and RICHARD N. KYLE

COLLEGE OF ENGINEERING
UNIVERSITY OF KENTUCKY
LEXINGTON, KENTUCKY 40506

Abstract

An experimental investigation is presented of the continuous-flow foam fractionation of each of the divalent colligends, $HAsO_4^{2-}$, HPO_4^{2-}, SO_4^{2-}, and SeO_3^{2-}, versus Br^-, the counterion of the ethylhexadecyldimethylammonium cation, over the 10^{-4}–10^{-3} M concentration range. Initial experiments with SeO_3^{2-} confirm the achievement of a single-equilibrium-stage separation. Selectivity coefficients, defined in terms of a colligend–surfactant counterion interaction model at the interfaces of the rising gas bubbles and in terms of the exchange of the surfactant counterion with the monovalent complex anion hypothesized to form between the surfactant cation and the divalent colligend, are established. They represent the ratio of colligend to bromide in the interfacial "stream" at unit ratio in the residual stream and are as follows: HPO_4^{2-}, 1.77; $HAsO_4^{2-}$, 1.59; SO_4^{2-}, 1.06; and SeO_3^{2-}, 0.97. A selectivity sequence is presented for 15 oxyanion and halide colligends. A single equation is developed to correlate the surfactant separation in the presence of any of 10 monovalent or divalent colligends, taking into account ionic strength effects. The surfactant separation equation and selectivity coefficients can be used to compute the colligend separation achieved in a single-equilibrium-stage foam fractionation.

INTRODUCTION

Foam fractionation processes have been used extensively to concentrate and to remove selectively nonsurface-active ions from dilute (10^{-6}–10^{-3} M) aqueous solutions. An ionic surfactant interacts preferentially with the ion of interest, termed the colligend, in competition with ions of like charge (including the surfactant's counterion). The surfactant–colligend ion pairs or

soluble complexes (no particles are formed) are concentrated in the foam which is formed by the passage of gas bubbles through the bulk solution. Foam fractionations have been included in recent reviews (*1, 2*) of foam separation processes, updating earlier reviews (*3–6*). The most simple and convenient mode of operation, which yields consistent, reproducible, and readily-interpretable separation data, is a continuous-flow, steady-state, single-equilibrium-stage unit.

A rather useful way to describe a foam fractionation is in terms of a dimensionless selectivity coefficient which is defined on the basis of the hypothesis made concerning the colligend–surfactant interaction which occurs. For monovalent colligends, a model based on colligend–surfactant counterion exchange at the interfaces of the rising gas bubbles has been validated in comparison with other possible interaction models (*7*). Selectivity coefficients from this model have been reported for monovalent colligends (*8–10*) and for a few divalent colligends (*11, 12*).

The objectives of this investigation are (a) to determine if the experimental, continuous-flow unit in fact produces a single-equilibrium-stage separation for a surfactant and divalent colligend; (b) to establish if, for a series of divalent oxyanions, the monovalent complex anion formed between the colligend and the surfactant cation is the exchanging species; (c) to determine experimentally accurate and reproducible values of the selectivity coefficients for $HAsO_4^{2-}$, HPO_4^{2-}, SO_4^{2-}, and SeO_3^{2-}, each versus Br^-, the counterion of the ethylhexadecyldimethylammonium cation ($EHDA^+$); (d) to utilize these coefficients to compile and report a complete selectivity sequence for 15 monovalent and divalent oxyanions and halides; and (e) to develop a correlation to enable the calculation of the surfactant separation, applicable in the presence of each of the colligends, which can be utilized in conjunction with the selectivity coefficients to calculate the single-equilibrium-stage colligend separation.

COLLIGEND–SURFACTANT INTERACTION MODEL AND SELECTIVITY COEFFICIENTS

A schematic diagram of a continuous-flow, single-equilibrium-stage foam fractionation unit is presented in Fig. 1. The feed stream from the mix tank to the column contains concentrations e_i of the ethylhexadecyldimethylammonium ($EHDA^+$) cation; b_i of $EHDA^+$'s counterion, Br^-; n_i of the cation of the colligend salt, Na^+; and c_i of the colligend anion, either $HAsO_4^{2-}$, HPO_4^{2-}, SO_4^{2-}, or SeO_3^{2-}, with all concentrations in mole/liter. The flow rate of the feed stream is L, liter/min; and flow rate of the gas stream is A,

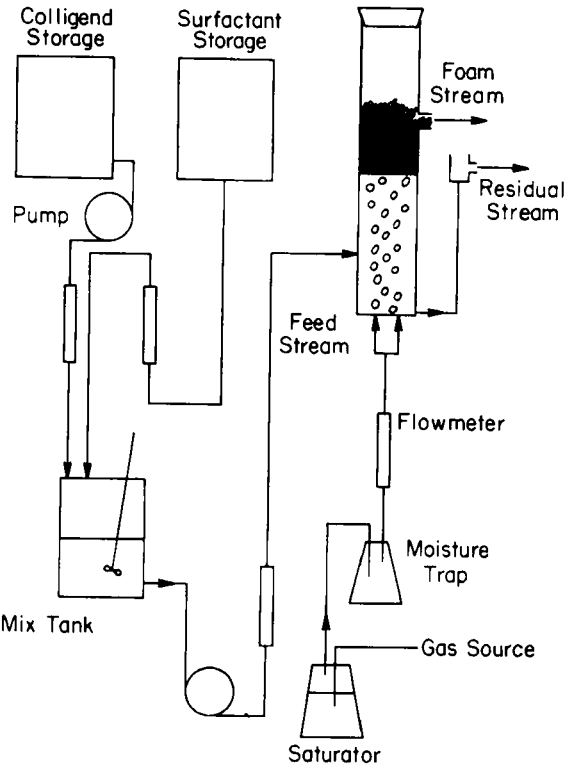

FIG. Schematic diagram of continuous-flow, single-equilibrium-stage foam fractionation unit.

cm^3/min; and the average bubble diameter is D_b, cm. The steady-state foam stream (collapsed, as liquid) contains the concentrations e_f, b_f, n_f, and c_f of the four ionic species, respectively, and similarly for the residual or bulk stream, the steady-state concentrations are e_r, b_r, n_r, and c_r, respectively. As the gas bubbles rise through the bulk solution, the surfactant rapidly diffuses to the gas–solution interfaces, and for a single equilibrium stage, the surface excess of surfactant in the interfacial fraction of the foam liquid (or interfacial "stream"), Γ_e, is in equilibrium with e_r.

Based on several key assumptions (*7*) which have been verified experimentally (*8*), the following mass balance equations may be written for the column:

$$\Gamma_e = \frac{D_b L}{6A}(e_i - e_r) = k'(e_i - e_r) \qquad (1)$$

$$\Gamma_b = \frac{D_b L}{6A}(b_i - b_r) = k'(b_i - b_r) \tag{2}$$

$$\Gamma_c = \frac{D_b L}{6A}(c_i - c_r) = k'(c_i - c_r) \tag{3}$$

in which Γ_e, Γ_b, and Γ_c are the surface excesses of surfactant, bromide, and colligend, respectively, in mol/cm^2, and k' is a procedure dependent "constant" which will be detailed in the Results and Discussion section. Experiments have shown clearly (*8, 13*) that sodium is neither positively nor negatively adsorbed at the gas–solution interface and therefore, Γ_n, the surface excess of sodium, is zero. Accordingly, by an ion balance on the interfacial "stream" and from Eqs. (1)–(3),

$$\Gamma_e = \Gamma_b + 2\Gamma_c \tag{4}$$

$$(e_i - e_r) = (b_i - b_r) + 2(c_i - c_r) \tag{5}$$

Of the various possible models for colligend–surfactant interaction, the most valid for monovalent colligends is that based on colligend–surfactant counterion exchange at the interfaces of the rising gas bubbles (*7*). For divalent colligends, the model hypothesizes that the surfactant cations rapidly diffuse to and are adsorbed at the gas–solution interfaces and behave as mobile anion exchangers, according to the following "reaction" (*11, 12*),

$$2(\text{EHDA–Br})_s + (SO_4^{2-})_r \rightleftharpoons (\text{EHDA}_2\text{–}SO_4)_s + 2(Br^-)_r$$

where the subscripts s and r indicate the interfacial or surface "stream" and residual stream (bulk solution), respectively. For a single-equilibrium-stage foam fractionation, and from Eqs. (2) and (3), the surface-exchange reaction equilibrium constant, which is also a surfactant selectivity coefficient, may be written (neglecting activity coefficient contributions),

$$K_{se} = \frac{[\text{EHDA}_2\text{–}SO_4]_s [Br^-]_r^2}{[\text{EHDA–Br}]_s^2 [SO_4^{2-}]_r} = \left(\frac{\Gamma_c}{c_r}\right) \Big/ \left(\frac{\Gamma_b}{b_r}\right)^2$$

$$= \left(\frac{c_i - c_r}{c_r}\right) \Big/ \left(\frac{b_i - b_r}{b_r}\right)^2 \tag{6}$$

To write the last section of Eq. (6), utilizing Eqs. (2) and (3), k' must be combined with K_{se} to form a new "constant." Because L, A, and D_b and thus k' were held constant in this study, a different $K'_{se} = (K_{se})(k')$ need not be used herein.

An alternative exchange reaction is also possible. For a solution containing long-chain quaternary ammonium cations and divalent colligend anions (SO_4^{2-}, for example), it is possible that all of the colligend is immediately paired as EHDA–SO_4^-. The surface exchange reaction which then occurs is

$$(\text{EHDA–Br})_s + (\text{EHDA}-\text{SO}_4)_r \rightleftharpoons (\text{EHDA}_2\text{–SO}_4)_s + (\text{Br}^-)_r$$

and the selectivity coefficient is

$$K_{se} = \frac{[\text{EHDA}_2\text{–SO}_4]_s[\text{Br}^-]_r}{[\text{EHDA–Br}]_s[\text{EHDA–SO}_4^-]_r} = \left(\frac{\Gamma_c}{c_r}\right) \Big/ \left(\frac{\Gamma_b}{b_r}\right)$$
$$= \left(\frac{c_i - c_r}{c_r}\right) \Big/ \left(\frac{b_i - b_r}{b_r}\right) \tag{7}$$

Equations (6) and (7) may be written

$$\frac{c_i - c_r}{c_r} = K_{se}\left(\frac{b_i - b_r}{b_r}\right)^n \tag{8}$$

with the best values of n and K_{se} to be determined experimentally.

Other colligend–surfactant interaction models are possible, based on ion pair formation in the feed solution and no surface exchange or on surface exchange coupled with ion pair formation in the residual stream (bulk solution). These could not be validated for monovalent colligends (*7*), and dubious assumptions must be made for complete model development for divalent colligends (*14*).

EXPERIMENTAL

Apparatus and Procedure

A schematic diagram of the experimental unit is shown in Fig. 1. Surfactant and colligend solutions were prepared by dissolving the surfactant and salt in double distilled water with a conductivity of 5.5 μmho/cm at 25°C. The concentration of surfactant ranged from 1.0×10^{-4} to 3.0×10^{-4} M, and the concentration of the salt from 1.0×10^{-4} to 7.0×10^{-4} M. In some experiments, sodium bromide was mixed with the colligend salt to vary the colligend/bromide ratio in the feed solutions. The surfactant solution was allowed to flow by gravity at a rate of 0.006 L/min metered by a Matheson flow meter. The colligend solution to be studied was fed to the mixing tank by

a Cole-Parmer peristaltic pump at a rate of 0.05 L/min through a Matheson flow meter. These two streams were completely mixed by a Talboys mixer, with a detention time of 45–50 min. In most of the experimental runs the feed solution was pumped to the foam column at a rate of 0.056 L/min through a glass port at a height of 10 cm above the base of the column. Three other experimental runs were performed by introducing the feed stream at a height from 11.5 to 31.5 cm above the foam–solution interface, 44 to 64 cm above the base of the column.

The inside diameter of the cylindrical glass column was 9.7 cm, with an overall height 89.5 cm. In most cases the solution height in the column was maintained at 32.5 cm. Foam exited through a side port 1.7 cm in diameter and 11.5 cm above the foam–solution interface A few experiments were run at a solution height of 32.5 to 62.5 cm and a foam height of 11.5 to 41.5 cm above the foam–solution interface. The residual stream exited via an outlet port at the base of the column. The residual flow rate was determined by collecting a volume of flow over a 10-min period. Residual stream flow rates averaged 0.0542 L/min for all runs.

Nitrogen was saturated by bubbling through distilled water and a moisture trap and then was dispersed into the column through twin sintered glass diffusers of 0.005 cm porosity and 3.0 cm diameter at a rate of 400 cm^3/min. Bubble diameters were found by an experimental technique. Pictures of at least 100 bubbles were taken with a Nikon Model F camera (lens 1:3.5, $f = 50$ mm), Kodak Tri-X Pan film, and a Strobotac flash unit. A fine wire of known diameter was placed in the column and included in the picture. The average bubble diameter was approximated from $D_b = \Sigma n_j D_{bj} / \Sigma n_j$ and was 0.055 cm with a standard deviation of 0.023 cm.

The system reached steady state in a shorter time if the column was filled with a surfactant–colligend solution of the concentration expected in the residual stream at steady state. Each run was carried out for 2 to $2\frac{1}{2}$ h. Samples of the residual stream were taken at 15 min intervals. When the concentrations of three consecutive samples were within at least 5%, the column was considered to be at steady state. Foam was periodically collected to check for flow rate and particle formation.

In the monohydrogen phosphate runs, 10 mL/L of 1.0 *N* NaOH were added to the colligend storage tank to maintain a pH of 10.5 ± 0.3 units in the mix tank. This pH was needed to insure that HPO_4^{2-} was the predominant species (*15*). For the arsenate and selenite systems, the pH values were adjusted to 9.0 ± 0.3 and 10.3 ± 0.3, respectively, by adding corresponding NaOH solution. This would make $HAsO_4^{2-}$ and SeO_3^{2-} the predominant species (*16*). For the above three systems, the pH values of the feed and residual streams were found to be constant and identical over the experimental runs, indicating no adsorption of OH^- at the interface.

Reagents and Analysis

The surfactant was Eastman ethylhexadecyldimethylammonium bromide, which analyzed 99.3% active on a bromide basis and 93.0% active on a carbon basis. The surfactant in the residual stream was analyzed with a Beckman total carbon analyzer. Bromide was analyzed by ultraviolet absorption at 198 nm with a Beckman DBG spectrophotometer. The bromide concentration in the residual stream could not be determined in the presence of phosphate or selenite, and for these series of runs the bromide concentration was established from Eq. (5).

The colligend reagents and modes of analysis were as follows:

Sodium sulfate, Baker, 99.9%; analyzed by direct titration with 0.005 M $BaCl_2$, using thorin as the indicator, in 80% ethanol with pH in the range 2.5–4.0.

Sodium phosphate (dibasic), Allied, 99.0%; analyzed by ultraviolet absorption at 400 nm with a vanadate-molybdate reagent.

Sodium arsenate, Fisher, 99.0%; determined with a Varian atomic absorption spectrophotometer, carbon rod, wavelength 193.6 nm, absorption coefficient of 0.342 per 5.0×10^{-5} M arsenate.

Selenous acid, Baker, 93.2%; determined by atomic absorption, carbon rod, wavelength 196.0 nm, absorption coefficient of 0.440 per 5.0×10^{-5} M selenite.

The accuracy of all the analyses was in the 4–5% range at the concentration levels employed in the foam fractionations. In several experiments the sodium concentrations in the feed and residual streams were analyzed by atomic absorption and were found to be consistently equal, validating the assumption made in writing Eqs. (4) and (5) of no positive or negative adsorption of Na^+ at the gas–solution interfaces.

RESULTS AND DISCUSSION

An initial series of experiments was carried out with SeO_3^{2-} as the colligend to test the validity of the assumption of single-equilibrium-stage operation, with results presented in Table 1. In these experiments and all others described for the colligends $HAsO_4^{2-}$, HPO_4^{2-}, SO_4^{2-}, and SeO_3^{2-}, the operational variables L, A, and D_b appearing in Eqs. (1)–(3) were 0.056 L/min, 400 cm^3/min, and 0.056 cm, respectively. Therefore, k' in Eqs. (1)–(3) was 1.3×10^{-6} L/cm^2 and $\Gamma_e = 1.3 \times 10^{-6}\,(e_i - e_r)$, etc.

From Table 1 it is clear that the solution height had no significant effect either on surfactant adsorption or colligend adsorption at the gas–solution

TABLE 1

Effects of Solution Height, Foam Height, and Feed Position Height on the Foam Fractionation of SeO_3^{2-}

$e_i = b_i \doteq 2.0 \times 10^{-4} M$

$c_i \doteq 2.0 \times 10^{-4} M$

Solution height above column base (cm)	Foam height above foam–solution interface (cm)	Feed position height above		$(e_i - e_r) \times 10^4$ (M)	$(c_i - c_r) \times 10^4$ (M)
		Base	Interface		
32.5	11.5	10.0	—	1.10	0.31
52.5	11.5	10.0	—	1.16	0.34
62.5	11.5	10.0	—	1.08	0.33
32.5	11.5	10.0	—	1.10	0.31
32.5	31.5	10.0	—	1.20	0.33
32.5	41.5	10.0	—	0.94	0.28
32.5	41.5	10.0	—	0.94	0.28
32.5	41.5	44.0	11.5	1.39	0.58
32.5	41.5	54.0	21.5	1.30	0.53
32.5	41.5	64.0	31.5	1.14	0.31

interfaces. Evidently the surfactant diffused rapidly to the interfaces of the rising gas bubbles, resulting in equilibrium adsorption, and the surface exchange reaction between Br^- and SeO_3^{2-} had reached equilibrium by the time the bubbles rose to the lowest solution height of 32.5 cm. From the second section of Table 1, there was no significant effect of foam height (at a constant solution height of 32.5 cm) over the 11.5–31.5 cm range, indicating minimum bubble coalescence and that the liquid draining from the foam was of concentration e_r, b_r, and c_r in $EHDA^+$, Br^-, and SeO_3^{2-}, respectively. However, the sharp decline over the 31.5–41.5 cm range indicates some bubble coalescence and the return of some of the rich interfacial liquid to the residual stream. The position of the feed to the column (the third section of Table 1) was varied purposefully in an effort to depart from single-equilibrium-stage operation. When the feed was introduced into the foam, the sharp increases in $e_i - e_r$ and in $c_i - c_r$ were produced by multiple stage stripping, with the decline at the highest feed position produced by extensive bubble coalescence.

Table 1 validates the assumption of single-equilibrium-stage operation at a solution height of 32.5 cm, foam height of 11.5 cm, and feed position of 10.0

cm: all additional experiments were conducted at these levels of the variables.

A second, rather extensive series of foam fractionation experiments (53 runs) was carried out to establish n and K_{se} in Eq. (8) for a sequence of divalent colligends which are commonly encountered, for which selectivities have not been reported in a thorough and complete fashion, and of which the principal elements occupy neighboring positions in the Periodic Table. Table 2 presents a summary of the experimental conditions. For the sake of completeness, data are reviewed (*11*) for CrO_4^{2-} and $S_2O_3^{2-}$; these colligends had been foam fractionated with the same surfactant at virtually the same experimental conditions.

To determine the best n in Eq. (8), values of $(c_i - c_r)/c_r$ and $(b_i - b_r)/b_r$ were computed for each run and were analyzed by a least squares analysis. The logarithmic relationships for $HAsO_4^{2-}$ and HPO_4^{2-} are presented as examples in Figs. 2 and 3 (solid lines) and the best values of n are summarized for all six colligends in the second column of Table 3. For all the colligends, n ranged from slightly greater than 1.0 to less than 1.0, indicating that the hypothesis leading to Eq. (7) (monovalent complex anion exchange with Br^-) is clearly better than the hypothesis leading to Eq. (6) (divalent anion exchange with Br^-). This conclusion had also been reached for other divalent colligends (*11*, *12*). The analysis was then repeated for each colligend, forcing $n = 1.0$ in Eq. (8) and yielding the dashed lines in Figs. 2 and 3. The best value of K_{se} at $n = 1.0$ for each colligend is presented in Table 3, together with the 95% confidence limits and r, the least squares correlation coefficient. The indicated confidence limits mean that if the assumptions made to develop Eq. (7) are correct, it can be stated with 95% confidence that the true value of K_{se} lies between the value in Table 3 plus the limit and the value in Table 3 minus the limit. The least squares correlation coefficient, r, is defined by

TABLE 2

Experimental Conditions for the Divalent Colligends

Colligend	Number of experiments	pH	Range of $e_i \times 10^4(M)$	Range of $b_i \times 10^4(M)$	Range of $c_i \times 10^4(M)$
$HAsO_4^{2-}$	13	9.0	1.0–3.0	1.0–3.1	1.0–7.0
HPO_4^{2-}	12	10.5	1.0–3.0	1.1–3.0	1.0–4.1
SO_4^{2-}	13	6.2	1.0–3.0	1.0–11.0	2.0–4.0
SeO_3^{2-}	15	10.3	1.0–3.1	1.1–10.0	1.0–5.2
CrO_4^{2-}	21	10.3	1.4–3.0	1.4–11.0	0.4–2.3
$S_2O_3^{2-}$	18	6.3	1.4–3.1	1.4–11.0	0.5–1.2

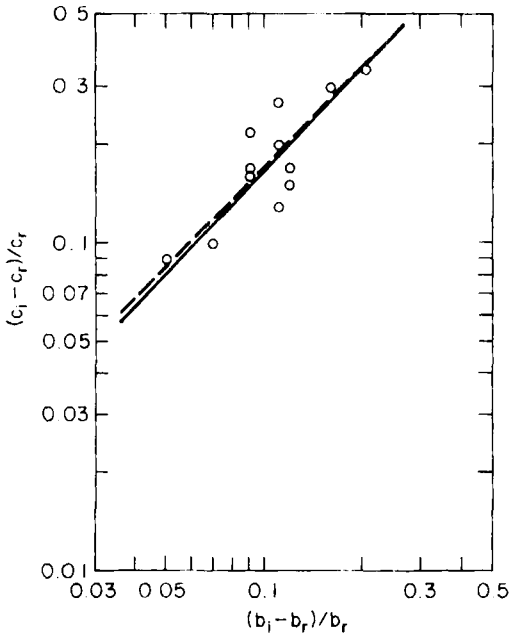

FIG. 2. Relationship between $(c_i - c_r)/c_r$ and $(b_i - b_r)/b_r$ (logarithmic coordinates) for $HAsO_4^{2-}$.

$$r = \left[1 - \frac{\Sigma[g_{\text{experimental}} - g_{\text{calculated}}]^2}{\Sigma[g_{\text{experimental}} - g_{\text{mean}}]^2}\right]^{1/2} \tag{9}$$

in which g stands for $(c_i - c_r)/c_r$ and the calculated values are computed from Eq. (8) with $n = 1.0$ and with K_{se} = the value in Table 3. With the possible exception of SO_4^{2-}, the correlation coefficients indicate a reasonable fit for Eq. (7); data sensitivity is discussed below.

An additional method of computing K_{se} is by plotting $(c_i - c_r)/(b_i - b_r)$ vs c_r/b_r, as indicated in Figs. 4 and 5 for $HAsO_4^{2-}$ and HPO_4^{2-}. The selectivity coefficient, K_{se}, is the slope of the best straight line through the data and through (0, 0) according to Eq. (7). The best values of K_{se}, confidence limits (dashed lines in Figs. 4 and 5), and correlation coefficients are presented in Table 4 for the six divalent colligends. The purpose of this second analysis is to give a balanced weighting to all of the data for each colligend: points with large values of $(c_i - c_r)/(b_i - b_r)$ and of c_r/b_r (Figs. 4 and 5) have small values of $(c_i - c_r)/c_r$ and of $(b_i - b_r)/b_r$ (Figs. 2 and 3), and vice versa. The values of K_{se} in the last column in Table 4 are the averages of the values

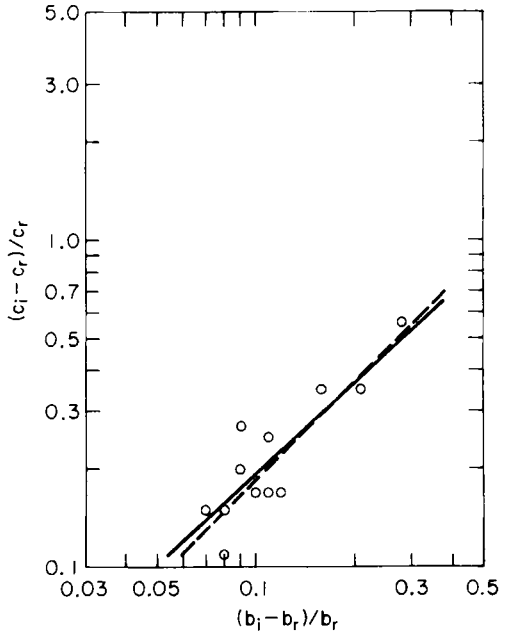

FIG. 3. Relationship between $(c_i - c_r)/c_r$ and $(b_i - b_r)/b_r$ (logarithmic coordinates) for HPO_4^{2-}.

established by the two methods of analysis and are the very best selectivity coefficients determinable from the data.

For each colligend the K_{se} gives the colligend/surfactant counterion (Br^-) ratio at the gas–solution interface (for a single equilibrium stage) as a linear function of the concentration ratio in the residual stream. If the complete separation is to be described for specified e_i, b_i, and c_i, Eq. (10), derived by substituting Eq. (5) in Eq. (7) to eliminate b_r, shows that c_r can be calculated from a knowledge of K_{se}, if e_r can be estimated:

$$K_{se} = \frac{(c_i - c_r)}{[(e_i - e_r) - 2(c_i - c_r)]} \Big/ \frac{c_r}{[2(c_i - c_r) - (e_i - e_r) + b_i]} \quad (10)$$

Surfactant adsorption at the gas–solution interface is generally described by an equation of the form

$$\Gamma_e = \frac{D_b L}{6A}(e_i - e_r) = me_r \quad (11)$$

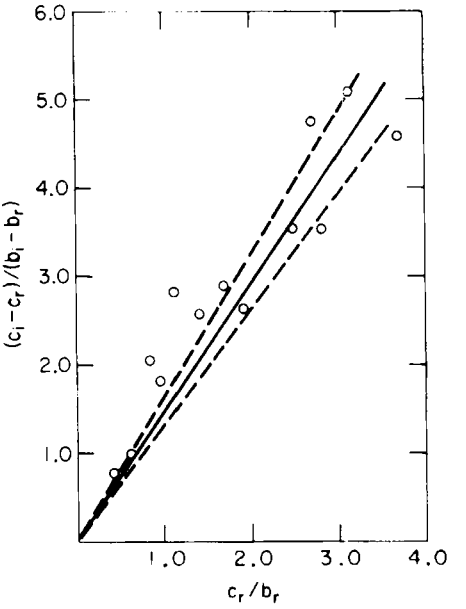

FIG. 4. Relationship between $(c_i - c_r)/(b_i - b_r)$ and c_r/b_r for $HAsO_4^{2-}$.

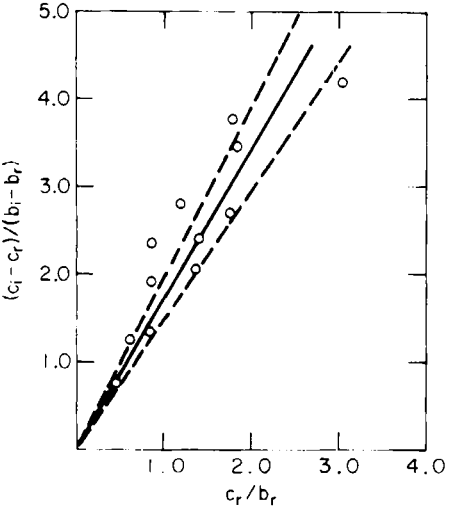

FIG. 5. Relationship between $(c_i - c_r)/(b_i - b_r)$ and c_r/b_r for HPO_4^{2-}.

TABLE 3

Values of Best n and Best K_{se} at $n = 1.0$ (for example, Figs. 2 and 3) for the Divalent Colligends

Colligend	Best n	K_{se} at $n = 1.0$	95% confidence limits for K_{se}	r for K_{se}
$HAsO_4^{2-}$	1.05	1.71	±0.20	0.86
HPO_4^{2-}	0.92	1.83	±0.21	0.90
SO_4^{2-}	0.76	1.16	±0.22	0.55
SeO_3^{2-}	0.60	0.86	±0.13	0.80
CrO_4^{2-}	0.80	3.85	±0.77	0.86
$S_2O_3^{2-}$	1.04	17.9	±2.7	0.92

or

$$\Gamma_e = \frac{D_b L}{6A}(e_i - e_r) = pe_r^a \tag{12}$$

or

$$\Gamma_e = \frac{D_b L}{6A}(e_i - e_r) = \frac{qe_r}{s + e_r} \tag{13}$$

in which m, p, a, q, and s are constants. Equation (13) is Langmuir's equation which also yields the approximate shape of the relationship between Γ_e and e_r predicted by Gibbs' equation. In Fig. 6, 31 data points are plotted for the single-equilibrium-stage foam fractionation of EHDA–Br, with each

TABLE 4

Values of Best K_{se} (for example, Figs. 4 and 5) and Average of Best K_{se} from Tables 3 and 4 for the Divalent Colligends

Colligend	K_{se}	95% confidence limits for K_{se}	r for K_{se}	Average best K_{se}
$HAsO_4^{2-}$	1.46	±0.16	0.89	1.59
HPO_4^{2-}	1.71	±0.24	0.85	1.77
SO_4^{2-}	0.96	±0.16	0.85	1.06
SeO_3^{2-}	1.08	±0.12	0.95	0.97
CrO_4^{2-}	3.96	±0.87	0.84	3.91
$S_2O_3^{2-}$	15.7	±3.9	0.83	16.8

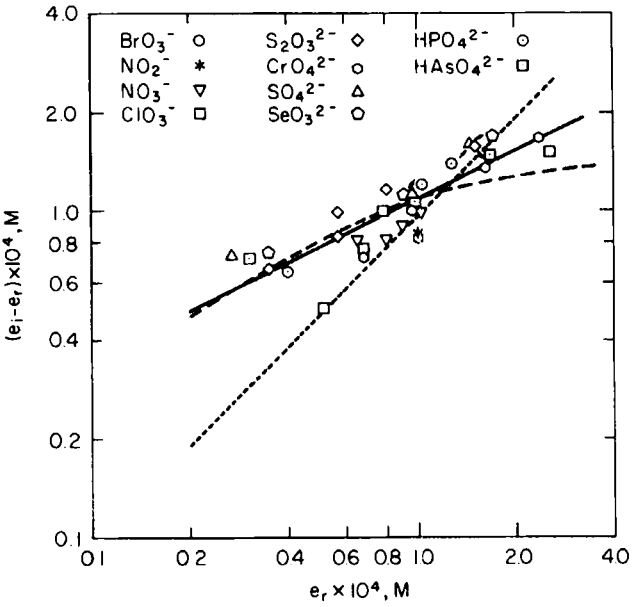

FIG. 6. Relationship between $(e_i - e_r)$ and e_r (logarithmic coordinates) for surfactant ethylhexadecyldimethylammonium bromide in presence of one of 10 colligends.

series of runs carried out in the presence of one of 10 colligends (*8, 11*). Each point is the average of from three to seven runs, with each run at constant e_i but variable c_i. The feed stream surfactant concentration was not varied over a wide range (1.0×10^{-4} to 4.0×10^{-4} *M*), but this was done purposefully to maintain D_b at a relatively constant value. Least squares analysis yielded

$$e'_i - e'_r = 0.941e'_r \tag{14}$$

or

$$e'_i - e'_r = 1.08(e'_r)^{0.485} \tag{15}$$

or

$$e'_i - e'_r = \frac{1.55e'_r}{0.462 + e'_r} \tag{16}$$

in which $e'_i = e_i \times 10^4$, $e'_r = e_r \times 10^4$, and with Eq. (16) determined from a linear plot of $1/(e'_i - e'_r)$ vs $1/e'_r$. Equations (14), (15), and (16) are indicated

in Fig. 6 by the dotted, solid, and dashed lines, respectively. The correlation coefficients, r, for Eqs. (14), (15), and (16) were 0.42, 0.87, and 0.77, respectively. Clearly, the linear dependence of Eq. (14) is not acceptable, Eq. (16) is acceptable but does not handle the points at high values of e'_r, and Eq. (15) gives a consistently good correlation.

If the 31 series of runs were combined with 35 points for similar experiments, but with NaBr added to the feed streams, then

$$e'_i - e'_r = 1.15(e'_r)^{0.534} \tag{17}$$

yielded a correlation coefficient of 0.89.

Equations (15) and (17) do not take into account the concentrations of colligend and of bromide in the feed streams, which seemingly should have some effect on surfactant adsorption due to variations in ionic strength. An increase in the ionic strength of a solution increases the relative polarity of the solution, and a hydrophobic surfactant will have a greater tendency to escape the solution to a gas interface. For a grand total of 167 runs (all of the runs from which the 31 average points in Fig. 6 were determined plus the 35 runs with added NaBr), stepwise multiple linear regression produced

$$e'_i - e'_r = 0.725(e'_r)^{0.406}(\mu')^{0.215} \tag{18}$$

in which μ' is the (ionic strength $\times 10^4$). The correlation coefficient, r, was 0.92 and the regression procedure indicated that μ' was a significant independent variable.

Equation (18) or Eq. (17) can be used with Eq. (10) at known values of e_i, b_i, and c_i to obtain a reliable estimate of the separation achieved. It should be noted here, and emphasized, that c_r (and b_r) are rather insensitive to changes in the values of K_{se}. Instead, K_{se} is very sensitive to changes in residual stream concentrations. For example, from Fig. 5 for HPO_4^{2-}, assume that for the point at $(c_i - c_r)/(b_i - b_r) = 2.44$, $c_r/b_r = 1.40$, $K_{se} = 1.73$ (the least squares line goes almost directly through this point), the measurement of c_r had been in error by 2%, with b_r to be adjusted correspondingly from Eq. (5). The coordinates of the point would shift to $(c_i - c_r)/(b_i - b_r) = 1.39$, $c_r/b_r = 1.52$, and the slope of the line from (0, 0) to that point would be 0.91, producing a change in K_{se} of 47%! This may account for some of the lower correlation coefficients in Tables 3 and 4, particularly the value in Table 3 for SO_4^{2-}. Due to the extreme sensitivity of K_{se} to the accuracy of the measurement of residual stream concentrations, it may be concluded that the model of Eq. (7) and the correlations of Figs. 2–5 and Tables 3 and 4 are reasonable.

SELECTIVITY SEQUENCE

Based on the results of these experiments for divalent oxyanions, and including CrO_4^{2-} and $S_2O_3^{2-}$, the following selectivity sequence can be written:

$$S_2O_3^{2-} \gg CrO_4^{2-} > HPO_4^{2-} \doteq HAsO_4^{2-} > SO_4^{2-} = Br^- = SeO_3^{2-}$$

The values of K_{se} in Table 4 may be compared to and combined with those for a series of monovalent oxyanions and halogens, the selectivity versus Br^- of each of which had been established in a single-equilibrium-stage unit with the surfactant ethylhexadecyldimethylammonium bromide: I^-, $K_{se} = 5.80$; ClO_3^-, 2.25; NO_3^-, 1.62; BrO_3^-, 0.96; NO_2^-, 0.73 (*7, 8*). Other studies (*8, 15, 17*) have provided information on $HCrO_4^-$, $H_2PO_4^-$, and Cl^-. The overall sequence can be written

$$\begin{aligned} HCrO_4^- &\gg S_2O_3^{2-} \gg I^- > CrO_4^{2-} > ClO_3^- > HPO_4^{2-} \doteq NO_3 \\ &= HAsO_4^{2-} > SO_4^{2-} = Br^- = Cl^- = SeO_3^{2-} \\ &= BrO_3^- > NO_2^- \doteq H_2PO_4^- \end{aligned}$$

Due to the identity of the expression for K_{se} for a monovalent colligend and of Eq. (7), the above, combined sequence may be written for monovalent and divalent species. However, one point of caution should be mentioned. If a monovalent colligend has the same K_{se} versus Br^- as a divalent colligend, then at the same c_r/b_r, each will have the same $(c_i - c_r)/(b_i - b_r)$ at the interface; but Eqs. (4), (5), and (10) will not be the same for the two colligends (the factor of 2 will disappear in each for the monovalent), and therefore for the same e_i, b_i, c_i, and e_r, different values of c_r will result for the two colligends.

CONCLUSIONS

(1) An experimental foam fractionation unit is shown to provide a single-equilibrium-stage separation of an ionic surfactant and a divalent colligend in competition with the surfactant's counterion. At the level of operating conditions utilized, the proportionality factor relating the surface excess to the difference between feed and residual stream concentrations is 1.3×10^{-6} L/cm^2.

(2) Based upon an interaction model hypothesizing colligend–surfactant counterion exchange at the gas–solution interfaces of the rising gas bubbles, an exchange reaction appears to occur for divalent colligends, with a monovalent, surfactant–colligend complex anion exchanging with Br^-. From

a careful statistical analysis of 53 experiments for four divalent colligends over the 10^{-4}–10^{-3} M concentration range, selectivity cofficients of 1.59, 1.77, 1.06, and 0.97 are determined for $HAsO_4^{2-}$, HPO_4^{2-}, SO_4^{2-}, and SeO_3^{2-}, respectively. These coefficients can be utilized together with those reported previously to produce a selectivity sequence of 15 monovalent and divalent oxyanions and halides.

(3) A single equation can be written to describe the surfactant separation achieved with each of 10 colligends, relating the residual stream surfactant concentration to the feed stream concentration and ionic strength. This equation can be used together with the selectivity coefficient for any of the colligends to calculate the overall separation achievable with a single equilibrium stage.

(4) The selectivity coefficients are very sensitive to data inaccuracies, and their reasonable constancy over the full concentration range indicates model verification. They provide a consistent and reliable method of reporting foam fractionation data.

REFERENCES

1. D. J. Wilson and A. N. Clarke, *Topics in Foam Flotation*, Dekker, New York, 1981.
2. R. B. Grieves, in *Treatise on Analytical Chemistry*, 2nd ed., Vol. 5 (P. J. Elving, ed.), Wiley-Interscience, New York, 1982.
3. R. A. Lemlich (ed.), *Adsorptive Bubble Separation Techniques*, Academic, New York, 1972.
4. S. F. Kuzkin and A. M. Golman, *Flotatsya Ionov i Molekul*, Atomizdat, Moscow, 1971.
5. P. Somasundaran, in *Separation and Purification Methods*, Vol. 1 (E. S. Perry and C. J. van Oss, eds.), Dekker, New York, 1973.
6. R. B. Grieves, W. Charewicz, and P. J. W. The, *Sep. Sci., 10,* 77 (1975).
7. R. B. Grieves and R. N. Kyle, *Sep. Sci. Technol., 17*, 465 (1982).
8. R. B. Grieves and P. J. W. The, *J. Inorg. Nucl. Chem., 36*, 1391 (1974).
9. R. B. Grieves, W. Walkowiak, and D. Bhattacharyya, in *Recent Developments in Separation Science*, Vol. V (N. N. Li, ed.), CRC Press, West Palm Beach, Florida, 1979.
10. W. Walkowiak and Z. Rudnik, *Sep. Sci. Technol., 13,* 127 (1978).
11. R. B. Grieves, R. L. Drahushuk, W. Walkowiak, and D. Bhattacharyya, *Sep. Sci., 11,* 241 (1976).
12. T. Gendolla and W. Charewicz, *Sep. Sci. Technol., 14,* 659 (1979).
13. W.-C. J. Chan, MS Thesis, University of Kentucky, Lexington, Kentucky, 1978.
14. R. N. Kyle, MS Thesis, University of Kentucky, Lexington, Kentucky, 1980.
15. R. B. Grieves and D. Bhattacharyya, *Sep. Sci., 1,* 81 (1966).
16. D. Bhattacharyya, M. Moffitt, and R. B. Grieves, *Sep. Sci. Technol., 13,* 449 (1978).
17. R. B. Grieves and T. E. Wilson, *Nature, 205*, 1066 (1965).

Received by editor July 27, 1981